molecular pharmaceutics

Article

pubs.acs.org/molecularpharmaceutics

Deeper Penetration into Tumor Tissues and Enhanced in Vivo Antitumor Activity of Liposomal Paclitaxel by Pretreatment with Angiogenesis Inhibitor SU5416

Yuta Yoshizawa,[†] Ken-ichi Ogawara,[†] Aya Fushimi,[†] Shigeki Abe,[†] Keisuke Ishikawa,[†] Tomoya Araki,[†] Grietje Molema,[‡] Toshikiro Kimura,[†] and Kazutaka Higaki*[,†]

[†]Department of Pharmaceutics, Faculty of Pharmaceutical Sciences, Okayama University, 1-1-1 Tsushima-naka, Kita-ku, Okayama 700-8530, Japan

[‡]Medical Biology section, Department of Pathology and Medical Biology, University Medical Center Groningen (UMCG), University of Groningen, Hanzeplein 1, 9713 GZ, Groningen, The Netherlands

ABSTRACT: The recently emerged concept of "vessel normalization" implies that judicious blockade of vascular endothelial growth factor (VEGF) signaling may transiently "normalize" the tumor vasculature, making it more suitable for tumor disposition of subsequently administered drugs. In this study, therefore, the effect of pretreatment with SU5416, a selective VEGF receptor-2 inhibitor, on tumor disposition and in vivo antitumor activity of polyethylene glycol (PEG)-modified liposomal paclitaxel (PL-PTX) was evaluated in Colon-26 solid tumor-bearing mice. To improve the solubility and in vivo disposition characteristics of SU5416, the inhibitor was formulated in PEGylated O/W emulsion (PE-SU5416). Pretreatment with PE-SU5416 significantly enhanced the in vivo antitumor effect of PL-PTX, although PE-SU5416 administration alone did not show any antitumor effect. Immunostaining for endothelial cells and pericytes demonstrated that the pretreatment with PE-SU5416 enhanced the pericyte coverage of the tumor vasculature. In addition, tumors treated with PE-SU5416 contained significantly smaller hypoxic regions compared with the nontreated control group, demonstrating that structural normalization of the tumor vasculature resulted in an improvement in tumor vessel functions, including oxygen supply. Furthermore, the pretreatment with PE-SU5416 increased the distribution of PEG liposomes and included PTX in the core region of the tumor, as well as conversely decreasing the ratio of their peripheral distribution. These results suggest that the structural and functional normalization of the tumor vasculature by the pretreatment with PE-SU5416 enabled liposomes to reach the deeper regions within tumor tissues, leading to more potent antitumor activity of PL-PTX.

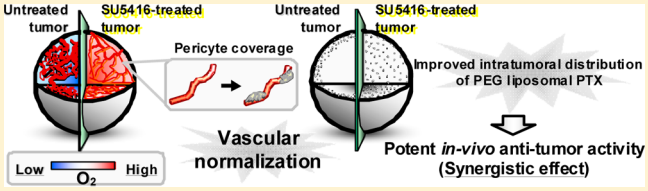

KEYWORDS: *drug delivery, PEG liposome, paclitaxel, VEGF, angiogenesis*

INTRODUCTION

It is known that a variety of pathophysiological features of solid tumors compromise the efficacy of conventional nonsurgical therapies.[1] Angiogenesis is one of the factors that need to be overcome to achieve efficient cancer chemotherapy. For the sustained growth of solid tumors, it is necessary for cancer cells to develop new capillaries from pre-existing blood vessels and to expand the vascular network to obtain oxygen and other nutrients.[2] However, due to the imbalance between pro- and antiangiogenic factors secreted in tumor tissues, the resulting tumor vasculature is structurally and functionally abnormal.[3−5] For example, vessel coverage by pericytes is generally poor in solid tumors, and the impaired pericyte coverage contributes to chaotic blood flow and excess permeability of the tumor vasculature. Furthermore, regions of severe oxygen deprivation (hypoxia) arise within solid tumors due to rapid division of tumor cells and aberrant blood vessel formation. These structural and functional abnormalities of the tumor vasculature cause spatial and temporal heterogeneous tumor blood flow.[6,7] In addition, proliferating cancer cells within tumor tissues generate internal high pressures, resulting in the impairment of blood flow due to the compression of intratumoral blood vessels.[8] These above-mentioned abnormalities in the tumor vasculature lead to a unique tumor microenvironment characterized by hypoxia, low pH, and elevated interstitial fluid pressure (IFP).[9] Specifically, from the therapeutic point of view, impaired blood supply and elevated IFP pose a barrier against delivering therapeutics to solid tumors.[10]

Jain et al. proposed that judicious attenuation of proangiogenic (VEGF) signaling, within a dose- and time-dependent schedule, may selectively prune immature blood vessels and remodel others. The resultant vasculature is less chaotic with greater pericyte coverage and reduced hyperpermeability, resembling that of normal tissue (vessel normalization).[10] These structural and functional transformations are further

Received: June 11, 2012
Revised: October 30, 2012
Accepted: November 7, 2012
Published: November 7, 2012

thought to be accompanied by physiological normalization of parameters such as decreased IFP and improved blood flow, leading to tumor oxygenation. These changes are considered to make the overall vascular network more stabilized and better suited to drug delivery.[10,11]

To date, a number of VEGF inhibitors have become available, including neutralizing anti-VEGF antibodies and small molecular weight compounds inhibiting VEGF receptor tyrosine kinase activity.[12] The concept of "vessel normalization" has already been confirmed by using various VEGF inhibitors such as bevacizumab,[13] sorafenib,[14] TSU68 (SU6668),[15] pazopanib,[16] DC101 (VEGF receptor-2 antibody),[17,18] and SU5416[19] in terms of the structural and functional transition of tumor vasculature. However, there are only a few reports addressing the antitumor effect of subsequently injected anticancer drugs after pretreatment with these VEGF inhibitors.[13,19]

In the present study, we selected SU5416, a hydrophobic molecule with potent tyrosine kinase inhibitory activity toward VEGF receptor-2 (VEGFR-2).[20] Other groups have already used this compound and demonstrated that structural and functional transition of the tumor vasculature could be achieved by treatment with this compound.[19] In those studies, due to its poor water solubility and poor tumor disposition, SU5416 was dissolved in DMSO or Cremophor EL, which are known to provoke undesirable side effects such as anaphylactic shock or hemolysis,[21] and it was administered as a peritoneal injection frequently at high doses.[19,22−24] To prepare safer dosage forms with better tumor targeting properties, we formulated SU5416 in polyethylene glycol (PEG)-modified O/W emulsion (PE-SU5416) and evaluated the effect of pretreatment with PE-SU5416 on tumor disposition and in vivo antitumor efficacy of subsequently administered PEG liposomal paclitaxel (PL-PTX) developed by our group[25] in Colon-26 (C26) solid tumor-bearing mice.

EXPERIMENTAL SECTION

Materials. Egg yolk phosphatidylcholine (EPC), Tween 80, tricaprylin, cholesterol (Chol), RPMI-1640, fetal bovine serum (FBS), and penicillin−streptomycin solution were purchased from Sigma (St. Louis, MO, USA). Gentamicin was purchased from Gibco BRL, Co. (Grand Island, NY, USA). Distearoyl phosphatidylethanolamine-*N*-[methoxy poly(ethylene glycol)-2000] (PEG-DSPE) and hydrogenated soybean phosphatidylcholine (HSPC) were purchased from NOF Inc. (Tokyo, Japan). SU5416 and paclitaxel (PTX) were kindly gifted from Taiho Pharmaceutical Co., Ltd. (Tokushima, Japan) and Sawai Pharmaceutical Co., Ltd. (Osaka, Japan), respectively. [^{3}H]-Cholesteryl hexadecyl ether (^{3}H-CHE) and PTX [2-benzoyl ring(U)-^{14}C] (^{14}C-PTX) were purchased from Perkin-Elmer Life Science Inc. (Boston, MA, USA) and Moravek Biochemicals Inc. (Brea, CA, USA), respectively. DiI (1,1′-dioctadecyl-3,3,3′,3′-tetramethylindocarbocyanine perchlorate) was purchased from Invitrogen (Paisley, U.K.). All other chemicals were commercial products of the finest grade.

Cells. Colon-26 carcinoma cells (C26) were kindly provided by the Cell Resource Center for Biomedical Research, Institute of Development, Aging and Cancer, Tohoku University (Sendai, Japan). C26 were cultured in RPMI-1640 supplemented with 10% heat-inactivated FBS, 2 mM L-glutamine, 100 U/mL penicillin, 100 μg/mL streptomycin, and 20 μg/mL gentamicin at 37 °C under 5% CO_2/95% air.

Preparation of SU5416-Encapsulated PEGylated O/W Emulsions (PE-SU5416). PEGylated O/W emulsion of SU5416 was prepared based on the method reported previously with minor modifications.[25] In brief, EPC, Tween 80, tricaprylin, and SU5416 (160:120:400:6.8, weight ratio) and PEG-DSPE (5 mol %) were dissolved in chloroform. Then, the oil phase was dried under reduced pressure at 50 °C. The aqueous phase composed of 2.25% (w/v) glycerol was mixed with the oil phase, followed by the sonication for 30 min at 4 °C using a probe-type sonicator (50 W, Ohtake Works, Tokyo).

Preparation of Paclitaxel-Encapsulated PEGylated Liposomes (PL-PTX). PEGylated liposomes containing PTX were prepared by the thin-film hydration method as reported previously.[25] In brief, HSPC, Chol, PEG-DSPE, and PTX (90:10:5:8, molar ratio) were dissolved in chloroform. To prepare radiolabeled PL-PTX for the evaluation of tumor disposition and intratumoral distribution of PEG liposomes and PTX, tracer amounts of ^{3}H-CHE and ^{14}C-PTX were further added to the mixture. For the preparation of DiI-labeled PEG liposomes, 1 mol % DiI was added to the lipid mixture as a fluorescent marker. After evaporation of the solvent at 75 °C, the lipid mixture was dried in vacuo at room temperature overnight. The resultant dried lipid film was hydrated with phosphate-buffered saline (PBS, pH 4.0) under mechanical agitation. The obtained multilamellar preparations were sized by repeated extrusion through polycarbonate membrane filters (Millipore, Bedford, MA) with a pore size of 200 nm followed by further extrusion through polycarbonate membrane filters of 100 nm pore size. The resulting liposomes were passed through a Sephadex G-25 column (Amersham Biosciences, Uppsala, Sweden) equilibrated with PBS (pH 7.4) to change the pH of the external phase and remove nonencapsulated PTX. Reproducible entrapment efficacy into liposomes was determined to be approximately 34%.

Animals and Preparation of the Tumor-Bearing Mice Model. Male BALB/c mice (6−7 weeks) were purchased from Charles River Laboratories Japan Inc. (Yokohama). Animals, maintained at 25 °C and 55% humidity, were allowed free access to standard chow and water. To prepare tumor-bearing mice, 10^6 C26 cells were subcutaneously inoculated into the backs of the mice. Our investigations were performed after approval by the local ethics committee at Okayama University and in accordance with the Principles of Laboratory Animal Care (NIH publication 85-23).

In Vivo Antitumor Activity. When the tumor volume reached about 100 mm^3 after inoculation of C26 cells, PE-SU5416 (5 mg/kg as SU5416) or PL-PTX (1 mg/kg as PTX) was intravenously administered to the monotherapy groups. For the combination therapy group, PE-SU5416 (5 mg/kg) was intravenously administered when the tumor volume reached about 100 mm^3. Twenty-four hours later, PL-PTX was injected at 1 mg/kg as PTX, while saline was injected into the control group mice. The size of the tumor was measured every day with a caliper in two dimensions, and the tumor volume was calculated using the following equation:[26]

$$\text{tumor vol (mm}^3\text{)} = \text{longer diam} \times (\text{shorter diam})^2 \times 0.52 \quad (1)$$

The slope of the tumor volume−time curve, representing the growth rate of each tumor, was obtained from days 3 to 18 after injection. The T/C index of the growth rate for the in vivo therapeutic effect of the tumor-bearing mice model was

obtained by dividing the growth rate of the treatment group (T) by that of the saline-treated control group (C).

Effect of PE-SU5416 on Pericyte Coverage and Vessel Morphology. To detect vascular endothelial cells and pericytes within the same tumor section, dual immunostaining was performed. PE-SU5416 (5 mg/kg as SU5416) or saline was intravenously administered into tumor-bearing mice when the tumor volume reached about 400−500 mm^3. At 24 h after the injection, tumor tissues were excised from mice and snap-frozen in acetone. 10 μm thick sections of tumor tissues were prepared with a cryostat (CM1850, Leica Microsystems, Wetzlar, Germany) and fixed with acetone. These sections were incubated with a rat anti-mouse CD31 antibody (550274, BD Biosciences, San Jose, CA) used at 1:50 (v/v) dilution in PBS containing 5% FBS (blocking buffer). This was followed by incubation with a rhodamine isothiocyanate (RITC)-conjugated rabbit anti-rat IgG antibody (55764, MP Biomedicals LLC-Cappel Products, Solon, CA). Immunostaining of αSMA was performed using a VECTOR M.O.M. immunodetection kit (FMK-2201, Vector Laboratories, Inc., Burlingame, CA) according to the manufacturers recommended procedures. In brief, after blocking using a protein block solution provided within the kit, the sections were incubated with an anti-αSMA antibody (MS-113, Thermo Fisher Scientific, Inc., Yokohama) at 1:800 (v/v) dilution. Then, the sections were incubated with a biotinylated anti-mouse IgG reagent, followed by fluorescein avidin DCS. The sections were observed under a fluorescence microscope (Biozero BZ-8000, KEYENCE, Osaka), and the images obtained with different filters were afterward overlaid. The fluorescence-positive area in the core part of tumor tissues was quantified by a fluorescence microscope equipped with image analysis software (VH-H1A5, KEYENCE).

Immunostaining of Carbonic Anhydrase 9 (CA9) within Tumor Tissues. To prepare tumor sections, excised tumor tissues were processed by the same method as described in the section Effect of PE-SU5416 on Pericyte Coverage and Vessel Morphology. To visualize hypoxic regions within tumor tissues, immunostaining of CA9, the endogenous hypoxia-inducible factor (HIF)-1-regulated protein, was performed. In brief, the tumor sections were incubated with a rabbit anti-mouse CA9 antibody (sc-25600, Santa Cruz Biotechnology, Inc., Santa Cruz, CA) used at 1:200 (v/v) dilutions in blocking buffer. As a second antibody, fluorescein isothiocyanate (FITC)-conjugated goat anti-rabbit IgG antibody (BT-557, Biomedical Technologies Inc., Stoughton, MA) was used at 1:500 (v/v) dilutions. The sections were observed under a fluorescence microscope (Biozero BZ-8000). The fluorescence-positive area was quantified by a fluorescence microscope equipped with image analysis software (VH-H1A5). During the staining procedure, an isotype-matched primary antibody that did not recognize CA9 was also used as a negative control. Since the staining using the isotype-matched control antibody did not give any color on the specimen, we regarded the staining procedure as adequate.

Tumor Disposition Characteristics of Both PEG Liposomes and PTX. When the tumor volume reached about 400−500 mm^3, PE-SU5416 (5 mg/kg as SU5416) or saline was intravenously administered. Then, 24 h later, PL-PTX labeled with ^{3}H-CHE and ^{14}C-PTX was injected at 1 mg/kg as PTX. At 24 h after PL-PTX injection, tumor tissues were excised, rinsed with saline, and weighed. To solubilize the tumor tissues, Soluvable (PerkinElmer Inc., MA) was added and they were incubated for 2 h at 60 °C before the solubilized solution was neutralized by HCl. Then, a scintillation medium (Clear-sol II, Nacalai Tesque, Kyoto, Japan) was added to the samples, and radioactivity derived from [^{3}H] and [^{14}C] was simultaneously but separately measured in a liquid scintillation counter (TRI-CARB 2260XL, Packard Instrument Inc., Meriden, CT, USA).

Intratumoral Distribution of PL-PTX. To assess the intratumoral distribution pattern of PEG liposomes and PTX, their distributed amounts into peripheral and central parts of tumor tissues were quantitatively evaluated. At 24 h after the injection of PL-PTX (1 mg/kg as PTX) labeled with ^{3}H-CHE and ^{14}C-PTX, tumor tissues were excised from mice, snap-frozen, and separated into peripheral and central parts using a brain slicer (MB-A1-S, Muromachi Kikai Co., Ltd., Tokyo) and scalpel. As shown in Figure 4A, tumor tissues were first horizontally divided into three sections with the same thickness, providing upper, middle, and lower sections. Then, the middle section was vertically further divided into 4 × 4 grids, the four central compartments (2 × 2 grids) of the section were defined as the core part, and the rest including the upper and lower sections was defined as the peripheral part. To measure radioactivity, these fractions were processed as described in the section Tumor Disposition Characteristics of Both PEG Liposomes and PTX.

Distribution Pattern of DiI-Labeled PEG Liposomes. DiI-labeled PEG liposomes (40 μmol total lipids/kg) were intravenously injected at 24 h postadministration of PE-SU5416 (5 mg/kg as SU5416). At 24 h after injection, tumor tissues were excised from mice and snap-frozen. To prepare upper, middle, and lower sections of tumor tissues, excised tumor tissues were processed by the same method as described in the section Intratumoral Distribution of PL-PTX. The upper or lower section was defined as the peripheral region, and the center part in the middle section was defined as the core region. To visualize endothelial cells within each region of tumor tissues, CD31 immunostaining was performed. In brief, the tumor sections were incubated with a rat anti-mouse CD31 antibody (BD Biosciences) used at 1:50 (v/v) dilutions in a blocking buffer. As a second antibody, a fluorescein-conjugated goat anti-rat IgG antibody (Life Technologies) was used at 1:200 (v/v) dilutions. The sections were observed under a fluorescence microscope (Biozero BZ-8000).

Statistical Analysis. Results are expressed as the mean ± SD of three or more experiments. Analysis of variance (ANOVA) was used to test the statistical significance of differences among groups. Statistical significance in the differences of the means was determined using the Student's t-test or Dunnett's test for single or multiple comparisons of experimental groups, respectively.

■ RESULTS AND DISCUSSION

In Vivo Antitumor Activity of PL-PTX with or without Pretreatment with PE-SU5416. VEGF stimulates endothelial cell migration, proliferation, survival, permeability, and lumen formation[27] and is indispensable to the initiation of angiogenesis.[28] Given its importance in cancer and numerous other angiogenic disorders, VEGF has become a prime target for antiangiogenic therapy.[29,30] Apart from its pruning effects on pre-existing vessels and inhibiting effect on growth of new vessels, blockage of VEGF or its signaling pathways may also induce normalization of the tumor vasculature to make distribution of drug delivery devices more efficient.[10] In the present study, therefore, SU5416 was selected as a selective inhibitor of VEGFR-2, and the effect of pretreatment with PE-

SU5416 on liposomal PTX delivery to tumor tissue and the in vivo antitumor activity of PL-PTX was evaluated in C26 solid tumor-bearing mice.

Generally, most solid tumors possess unique pathophysiological characteristics that are not observed in normal tissues/organs, such as extensive angiogenesis, defective vascular architecture, and an impaired lymphatic drainage/recovery system. Therefore, nanoparticles that exhibit long-circulating properties are expected to be accumulated preferentially in many types of solid tumors due to the enhanced permeability and retention (EPR) effect.[31] In our previous study, PTX formulated into a PEG liposome (PL-PTX) made it possible for PTX to be distributed to tumor tissues efficiently based on the EPR effect, which led to a prominent in vivo antitumor effect.[25]

It is believed that antitumor activity of compounds with antiangiogenic activity like SU5416 partly depends on the starvation of tumor tissues due to reduced tumor blood flow.[32] Therefore, in the present study, the dose of SU5416 was carefully chosen since preadministered SU5416 may reduce regional tumor blood flow, leading to a decrease in the tumor disposition of subsequently administered nanoparticles due to an impaired EPR effect. In this study, we chose the dose of PE-SU5416, 5 mg/kg single dose, based on our preliminary study, where we found that the excessive dose of PE-SU5416, 5 mg/kg × 5 times, significantly decreased CD31-positive vessels (48 ± 13% of control, $p < 0.001$), reduced the tumor growth, and tended to decrease the tumor distribution of subsequently injected PEG liposomes (74 ± 41% of control), which would be presumably due to the impaired EPR effect. As a result, we reached the conclusion that 5 mg/kg single dose of PE-SU5416 would be an adequate dose that did not inhibit the tumor growth alone (Figure 1) and made it possible to avoid the impaired EPR effect due to the reduced regional blood flow within tumor tissues. Figure 1 also shows the growth curves of C26 tumors after intravenous injection of PL-PTX (1 mg/kg as PTX) with or without pretreatment with PE-SU5416 (5 mg/kg as SU5416). PL-PTX alone significantly inhibited tumor growth (256.7 ± 78.7 mm^3/day ($n = 5$), $p < 0.01$) compared with the control group (514.4 ± 49.5 mm^3/day ($n = 5$)). Furthermore, it is noteworthy that PL-PTX administration after the pretreatment with PE-SU5416 exhibited significantly more prominent inhibition of tumor growth (143.0 ± 48.9 mm^3/day as growth rate ($n = 5$), $p < 0.05$) compared with PL-PTX alone. Taken that the single dose of PE-SU5416 did not show a significant antitumor effect, the result clearly indicated that the combination use of PL-PTX with PE-SU5416 have provided a certain synergistic antitumor effect. During the experiment, the weight change was checked every other day and all the treatment groups showed similar increases in body weights compared with the control group, suggesting that no apparent side effects occurred in the treatment groups.

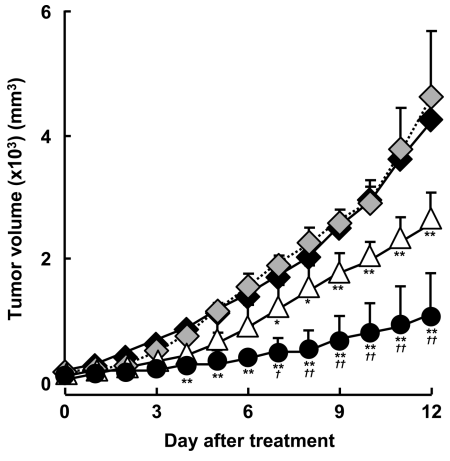

Figure 1. In vivo antitumor activity of PL-PTX with or without pretreatment with PE-SU5416. Saline or PE-SU5416 was injected on day 0, and PL-PTX was injected 24 h after administration of saline or PE-SU5416 (on day 1). Keys: closed diamond, control (saline); gray diamond, PE-SU5416; open triangle, PL-PTX; closed circle, PL-PTX after pretreatment with PE-SU5416. Each point represents the mean tumor volume with the vertical bar showing SD ($n = 5$). $^{**}p < 0.01$; $^{*}p < 0.05$, compared with saline-treated group. $^{\dagger\dagger}p < 0.01$; $^{\dagger}p < 0.05$, compared with PL-PTX alone.

Then, we tried to elucidate the mechanisms behind this synergistic antitumor effect of PE-SU5416 and PL-PTX by evaluating the effects of pretreatment with PE-SU5416 on the structural and functional properties of the tumor vasculature, since the concept of "vessel normalization" aims at making tumor vessels structurally and functionally closer to normal vessels. For these purposes, the following studies started when tumor volume reached 400−500 mm^3 because tumors that were large enough to investigate the intratumoral distribution of drugs and the morphology and function of tumor vessels were needed. However, we already confirmed that vessel density, assessed by CD31 staining, within tumors of 100 mm^3 (41.5 ± 7.5 vessel number/field) was similar to that within tumors of 400−500 mm^3 (46.8 ± 6.3 vessel number/field, not significant vs 100 mm^3) and that no necrotic regions were observed in either tumor in our preliminary study. Therefore, the two tumors were still in an early phase of tumor growth, and had similar phenotypes in their microenvironment.

Effect of PE-SU5416 on Pericyte Coverage of Vessels. First, to assess the effect of PE-SU5416 on vessel structure in the core part of tumor tissues, we performed immunofluorescence staining of CD31, a marker for vascular endothelial cells, within the tumor at 24 h after intravenous administration of PE-SU5416 (Figure 2). As shown in Figure 2A, it was found that the area of CD31-positive vessels (red) in the PE-SU5416-treated group tended to be lower compared with the control group, but the difference was not statistically significant ($p = 0.109$, Figure 2A,D), demonstrating that PE-SU5416 treatment attenuated tumor angiogenesis moderately. This result could possibly be related to the above-mentioned lack of antitumor effect of solely administered PE-SU5416 (Figure 1). Vessel coverage by pericytes (cells that provide support for the endothelial cells) is usually extensive in normal tissues with a slow endothelial cell turnover. It is known that impaired pericyte coverage contributes to chaotic blood flow and excess permeability of tumor vasculature.[33−35] Next, the area of αSMA-positive pericytes in tumors was also evaluated by immunostaining of αSMA (green), a marker for pericytes (Figure 2B), and found to be no different in both tumors (Figure 2B,E). On the other hand, CD31/αSMA-double positive area (yellow) was found to be larger in PE-SU5416-treated tumors than that in the control group (Figure 2C,F). Since the absolute number of vessels was slightly different between the control- and PE-SU5416-treated groups (Figure 2D), the index for pericyte coverage (ratio of pericyte-covered vessels (yellow) (Figure 2C) to CD31-positive vessels (red) (Figure 2A)) was also calculated and is shown in Figure 2F. The index was significantly increased in PE-SU5416-treated tumors compared with the control group (Figure 2F),

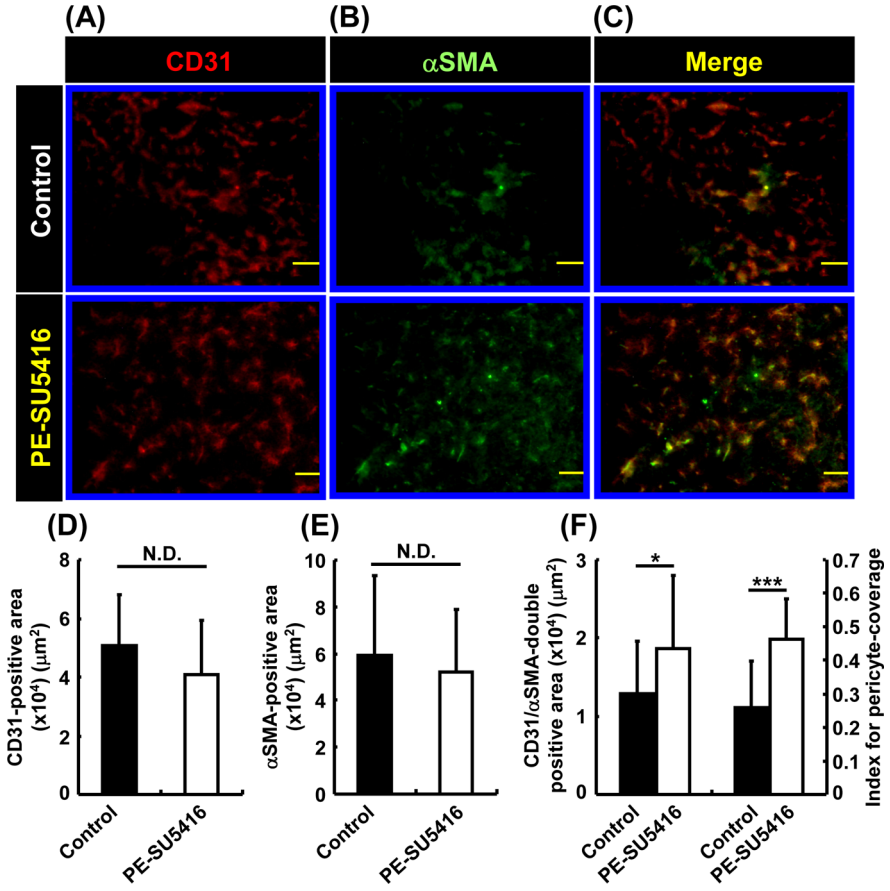

Figure 2. Effect of pretreatment with PE-SU5416 on structural properties of vessels within tumor tissue. Representative immunohistochemical staining images of (A) endothelial cells (CD31, red) and (B) pericytes (αSMA, green), and (C) merged images (pericyte-covered vessels, yellow) within tumor tissues. (D) The area of CD31-possitive vessels (red). (E) The area of αSMA-positive pericytes (green). (F, left) CD31/αSMA-double positive area (yellow). (F, right) The ratio of pericyte-covered vessels (yellow) to CD31-positive vessels (red). Results are expressed as the mean with the vertical bar showing SD (n = 20). ***p < 0.001; *p < 0.05, compared with control. Scale bars, 100 μm.

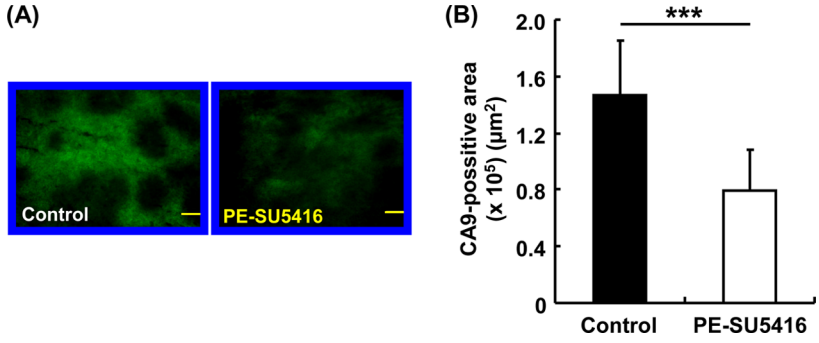

Figure 3. Immunohistochemical detection of hypoxic regions in PE-SU5416-treated and control tumors. (A) Representative immunostaining image of a hypoxic region (CA9-positive region, green). (B) The area of a hypoxic region within tumor tissues. Results are expressed as the mean with the vertical bar showing SD (n = 10). ***p < 0.001, compared with control. Scale bars, 100 μm.

demonstrating that PE-SU5416 treatment enhanced pericyte coverage of the tumor vasculature. In this study, we used αSMA as a pericyte marker. Since αSMA is also expressed in myofibroblasts or activated fibroblasts in tumor stroma,[36] the data should be carefully interpreted. Myofibroblasts or activated fibroblasts are located in tumor stroma being away from vessels.[36] Therefore, the αSMA-positive cells being away from vessels may also include myofibroblasts or activated fibroblasts in tumor stroma (Figure 2C), but the αSMA-positive cells adjacent to the vessel lumen, colocalizing with CD31-positive vessels, can be regarded as pericyte-covered vessels (Figure 2C,F). Our findings also coincide with the report that whereas blood vessels of control tumors were characterized by a loose and improper coverage by pericytes, blood vessels of SU5416-treated tumors demonstrated an intimate or more rigid pericytes−endothelial association.[37] These results indicate that, as a consequence of VEGFR-2 blockade by SU5416, pericytes were recruited to the microvessels and intensified their coverage, making tumor blood vessels more mature.

Effect of PE-SU5416 on the Function of Vessels. Second, we tried to assess the effect of PE-SU5416 treatment on the functional properties of the tumor vasculature. Since it is

dx.doi.org/10.1021/mp300318q | Mol. Pharmaceutics 2012, 9, 3486−3494

known that vessel normalization can be accompanied by improved tumor oxygenation,[10,11] we investigated the effect of pretreatment with PE-SU5416 on oxygen levels within tumor tissues, where immunostaining was performed for hypoxia-inducible factor-1 (HIF-1)-regulated protein CA9, a marker of hypoxic regions within tumor tissues.[38] In many types of tumors, structurally and functionally abnormal tumor vessels can easily extravasate intravascular fluids and plasma proteins. This excess extravasation of proteins increases the extravascular oncotic pressure, resulting in the interstitial hypertension within tumors.[39] This elevated IFP together with the mechanical stress from the solid mass of proliferating tumor cells located in the core region of tumor tissues and the extracellular matrix of tumor tissues are able to collapse tumor vessels, closing their lumen through compressive forces.[40] This vascular collapse due to elevated IFP hampers the efficient blood flow within tumor tissues and produces regional hypoxia and acidosis especially in the core region of tumor tissues.[41] As shown in Figure 3, tumors treated with PE-SU5416 contained significantly smaller hypoxic regions (CA9-positive regions) than those in the control group. The result suggests that part of tiny vessels in the core region of C26 tumor tissues would have been functionally insufficient due to the compressive pressure by elevating IFP and increasing the solid mass of tumor cells, and also suggests that PE-SU5416 would have improved oxygen supply into the core region of tumor tissues presumably due to the improvement of local blood flow. Although an increase in tumor oxygenation might not be necessarily associated with remodeling of tumor vasculature,[19] this functional improvement of vessels, together with the increase in the ratio of pericyte-covered vessels (Figure 2C,F), a structural maturation of vessels, would indicate the possible vessel normalization by PE-SU5416. However, the direct measurements of regional blood flow and IFP are of great importance to clarify these mechanisms, and these are the subjects of our further studies.

Possible Mechanisms Behind "Vessel Normalization" by PE-SU5416. Previous studies suggested that VEGF inhibition would cause vessel normalization, in part by the upregulation of angiopoietin-1 (Ang-1),[18] a matrix metalloproteinase which remodels the vascular basement membrane and surrounding matrix,[18] and activates platelet-derived growth factor receptor (PDGFR)-β signaling.[42] Ang-1 secreted by pericytes binds to the Tie2 receptor on endothelial cells, promotes vessel normalization, counteracts the VEGF-induced high vascular permeability by establishing tighter interendothelial junctions,[43,44] and favors tumor vessel maturation through pericyte recruitment.[45,46] PDGF-β, secreted by sprouting endothelial cells, is also a well-characterized recruitment signal for pericytes which express PDGFR-β.[47] Considering these factors, it can be speculated that VEGFR-2 blockade by PE-SU5416 activates Ang-1/Tie2 and PDGF-B/PDGFR-β signaling, leading to an improvement in pericyte coverage for tumor vessels (Figure 2). Contrary to this speculation, pretreatment with pazopanib, a novel multitargeted inhibitor of both VEGFRs and PDGFRs, was reported to reduce the number of pericyte-covered vessels and accordingly increased the area of the hypoxic region within tumor tissues.[16] Taken that pazopanib antagonizes the signal transduction of not only VEGFRs, including VEGFR-2, but also PDGFRs, and that PDGFR-β signaling is important for pericyte recruitment, the selective inhibition of VEGFR-2 with SU5416 would be a more suitable approach to achieve "vessel normalization". However, since the different doses of PE-SU5416 showed the different effects to microvessels within tumor tissues as described below, a lower dose of pazopanib may also have entirely different effects. Therefore, the theoretical benefits of inhibiting only the VEGFR2 pathway, rather than both the VEGFR2 and PDGFR pathways, should be carefully evaluated.

Effect of PE-SU5416 on Tumor and Intratumoral Distribution of PEG Liposomes and PTX. We next assessed the tumor disposition of both PEG liposomes and included PTX injected after the treatment with PE-SU5416. Although the pretreatment with PE-SU5416 slightly increased the tumor disposition of both PEG liposomes and PTX, there was no statistically significant difference between PE-SU5416-treated and control mice (PEG liposome, $p = 0.17$; PTX, $p = 0.21$). Although we speculated that the structural and functional normalization of tumor vessels would lead to enhanced tumor disposition of PL-PTX, the results obtained were not what we expected.

In order to clarify the mechanisms behind the synergistic antitumor effect of PE-SU5416 and PL-PTX, the effects of pretreatment with PE-SU5416 on intratumoral distribution of both PEG liposomes and PTX were evaluated (Figure 4). As shown in Figure 4B, intratumoral distribution of PEG liposomes in control tumors was exclusively limited to the peripheral region of tumor tissues. On the other hand, the pretreatment with PE-SU5416 increased the amount of PEG liposomes distributed to the core region of tumors and conversely reduced the ratio of its peripheral distribution. More importantly, the distribution of PTX included in liposomes in the core region was also significantly increased by the pretreatment with PE-SU5416 (Figure 4C). In addition, the extravasation of DiI-labeled PEG liposomes from the tumor vasculature was also assessed (Figure 5). The extravasation of PEG liposomes (red) from tumor vasculatures (green) was

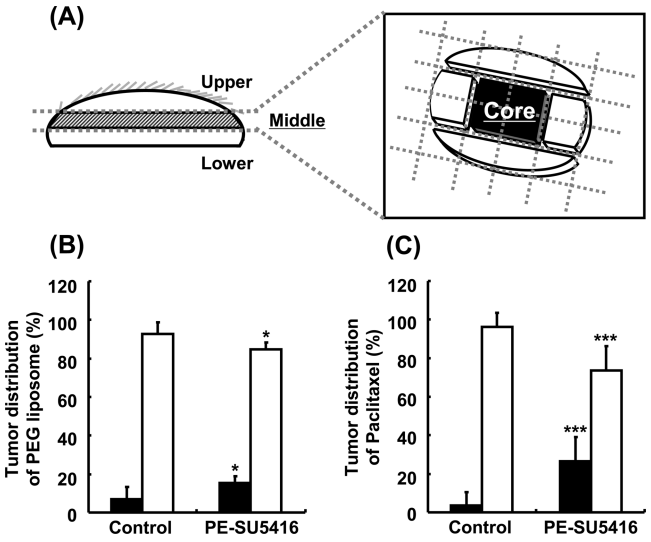

Figure 4. Effect of pretreatment with PE-SU5416 on intratumoral distribution of PL-PTX. Schematic representation of method to separate core and peripheral parts of tumor tissues (A). Details about how to separate the tumor tissues are described in the section Intratumoral Distribution of PL-PTX. Tumor disposition levels were separately measured for PEG liposomes (B) and paclitaxel (C) in the core and peripheral parts of tumor tissues using radiolabeled compounds. Keys: closed bar, core region; open bar, peripheral region. Results are expressed as the mean with the vertical bar showing SD ($n = 5$). ***$p < 0.001$; *$p < 0.05$, compared with control.

dx.doi.org/10.1021/mp300318q | Mol. Pharmaceutics 2012, 9, 3486−3494

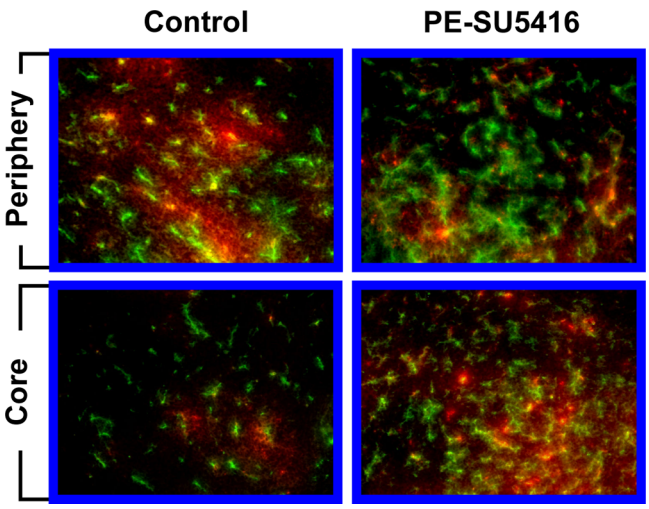

Figure 5. Distribution pattern of DiI-labeled PEGylated liposomes within core and peripheral regions of tumor tissues after pretreatment with PE-SU5416. Fluorescence staining was performed for CD31 at 24 h after the injection of DiI-labeled PEG liposomes. Representative image of extravasated DiI-labeled PEG liposomes (red) and endothelial cells (CD31, green) within tumor tissues.

observed exclusively in the peripheral region, and that in the core region was hardly observed in tumors excised from the nontreated control group. In the case of PE-SU5416-treated tumors, it was confirmed that the extravasation of PEG liposomes in the peripheral region did take place, but the extent was lower compared with that in the nontreated control group, presumably due to the reduced vascular permeability caused by pretreatment with PE-SU5416. On the other hand, the distribution and extravasation of PEG liposomes in the core region of tumor tissues were found to be larger in PE-SU5416-treated tumors than in the control group. These results were in good accordance with the quantification of the intratumoral distribution of PEG liposomes as shown in Figure 4. As described above, elevated IFP in the core part of tumor tissues impaired lymphatic drainage and hyperpermeability of the tumor vasculature,[9] and the elevated IFP suppresses convective transport of solutes, proteins, and blood cells, which would also be an obstacle for efficient drug delivery.[48] Supporting these results, a previous report demonstrated that the intratumoral distribution of PEG liposomal doxorubicin (Doxil) was limited exclusively to the tumor periphery.[16] In addition, it was reported that the treatment with an anti-VEGFR-2 antibody reduced tumor IFP and made it possible for bovine serum albumin (BSA) molecules to more deeply penetrate into tumors.[17,48] This would also be the case in the present study in which structural and functional normalization of tumor vessels by PE-SU5416 would reduce tumor IFP and extravascular oncotic pressure and improve regional blood flow within tumor tissues, leading to the enhancement of PL-PTX distribution to the deeper regions of tumor tissues. This speculation is partly supported by the results of CA9 staining, where the hypoxic region in the core part of tumor tissues significantly decreased (Figure 3).

Taken together, it is considered that vessel normalization by PE-SU5416 would make it possible for liposomes to reach deeper region of tumor tissues (Figures 4 and 5), leading to more potent antitumor activity of PL-PTX (Figure 1). This is the first report demonstrating that selective inhibition of the VEGFR-2 signal transduction pathway improved intratumoral distribution patterns of subsequently injected nanoparticles. In our previous report, PL-PTX made it possible for PTX to be distributed more efficiently to tumor tissues based on the EPR effect.[25] However, the present results suggest that distribution of PEG liposomes and PTX tends to be limited to the peripheral region of tumor tissues (Figure 4), and the poor intratumoral distribution patterns of PTX still attenuated the antitumor efficacy of PL-PTX.

For Further Optimization of the "Vessel Normalization" Strategy. To design an optimal combination therapy, we must further unravel the mechanism for the synergistic effect and time dependency of tumor vessel normalization and optimize the treatment schedule. Jain proposed that an optimal schedule for antiangiogenic therapy combined with chemotherapy and/or radiation therapy requires knowledge of the time window, termed as the "normalization window", during which the vessels initially become normalized, as well as an understanding of how long they remain in such a "normalized state".[10,49] A previous study, in which human tumors growing in nude mice were treated with an antibody to VEGFR-2, successfully clarified such a "normalization window", and the radiation therapy within the window yielded the best therapeutic outcome.[18] As described above, in our preliminary study, the excessive dose of PE-SU5416 (5 mg/kg × 5 times) at which CD31-positive vessels and the tumor growth significantly decreased, tended to reduce the tumor distribution of subsequently injected PEG liposomes, suggesting that angiogenesis inhibitors should be dosed at levels below the point at which they begin to strongly inhibit angiogenesis for the success of the "vessel normalization" strategy presented here. In this context, more detailed information on the optimum PE-SU5416 dose and treatment schedule including the initial tumor volume to start with the treatment will be necessary to further improve the in vivo efficacy of combination therapy with PL-PTX, which will be the subject of our further studies.

Another important issue is how to extrapolate the knowledge obtained in the present study to other types of solid tumors. In our previous study, C26 tumor cells were found to secrete large amounts of VEGF in the in vivo condition, and this was responsible for a large number of tiny vessels with high permeability.[50] This is the reason why the strategy described in this manuscript was successful for C26 tumor-bearing mice and the same strategy could be applicable for tumors with these phenotypes. Although the use of an orthotopic tumor model would have shown more benefit, the results obtained in murine ectopic tumor models presented in this study give new insight into the further optimization of combination therapy with antiangiogenic and anticancer drugs formulated in nanoparticles. A recently reported paper showed the size dependence of the vessel normalization strategy, in which blocking VEGF receptor-2 with an antibody hindered the delivery of 125 nm particles, but aided 12 nm particles.[51] The results shown in the article were different from ours, but one of the main reasons for it should be the difference in the type of tumor used. Since different types of tumors have blood vessels with different density and/or permeability,[50] the effect of "normalization" may also be dependent on the type of tumor. Therefore, a follow-up study using tumor cells with different phenotypes and using nanoparticles of different sizes will provide further information which will be of great importance to appreciate the potential of the "vessel normalization strategy" proposed here for future therapeutic application.

CONCLUSION

We here demonstrated that the selective inhibition of VEGFR-2 normalized the abnormal structure and function of tumor vasculature to provide more favorable intratumoral distribution of subsequently administered PEG liposomal PTX, leading to more effective in vivo antitumor activity in solid tumor-bearing mice. These findings indicate the potency of combination therapies using a VEGFR-2 inhibitor and anticancer agents in a judicious treatment schedule for the development of more efficient cancer chemotherapy.

AUTHOR INFORMATION

Corresponding Author

*Department of Pharmaceutics, Faculty of Pharmaceutical Sciences, Okayama University, 1-1-1 Tsushima-naka, Kita-ku, Okayama 700-8530, Japan. Tel: (+81)-86-251-7949. Fax: (+81)-86-251-7926. E-mail: higaki@pharm.okayama-u.ac.jp.

Notes

The authors declare no competing financial interest.

ACKNOWLEDGMENTS

We are grateful to Taiho Pharmaceutical Co., Ltd., and Sawai Pharmaceutical Co., Ltd., for kindly providing us with the drugs, SU5416 and paclitaxel, respectively.

REFERENCES

(1) Jain, R. K. Barriers to drug delivery in solid tumors. *Sci. Am.* **1994**, *271*, 58−65.

(2) Carmeliet, P.; Jain, R. K. Angiogenesis in cancer and other diseases. *Nature* **2000**, *407*, 249−257.

(3) Gazit, Y.; Baish, J. W.; Safabakhsh, N.; Leunig, M.; Baxter, L. T.; Jain, R. K. Fractal characteristics of tumor vascular architecture during tumor growth and regression. *Microcirculation* **1997**, *4*, 395−402.

(4) Morikawa, S.; Baluk, P.; Kaidoh, T.; Haskell, A.; Jain, R. K.; McDonald, D. M. Abnormalities in pericytes on blood vessels and endothelial sprouts in tumors. *Am. J. Pathol.* **2002**, *160*, 985−1000.

(5) Inai, T.; Mancuso, M.; Hashizume, H.; Baffert, F.; Haskell, A.; Baluk, P.; Hu-Lowe, D. D.; Shalinsky, D. R.; Thurston, G.; Yancopoulos, G. D.; McDonald, D. M. Inhibition of vascular endothelial growth factor (VEGF) signaling in cancer causes loss of endothelial fenestrations, regression of tumor vessels, and appearance of basement membrane ghosts. *Am. J. Pathol.* **2004**, *165*, 35−52.

(6) Yuan, F.; Leunig, M.; Huang, S. K.; Berk, D. A.; Papahadjopoulos, D.; Jain, R. K. Microvascular permeability and interstitial penetration of sterically stabilized (stealth) liposomes in a human tumor xenograft. *Cancer Res.* **1994**, *54*, 3352−3356.

(7) Campbell, R. B.; Fukumura, D.; Brown, E. B.; Mazzola, L. M.; Izumi, Y.; Jain, R. K.; Torchilin, V. P.; Munn, L. L. Cationic charge determines the distribution of liposomes between the vascular and extravascular compartments of tumors. *Cancer Res.* **2002**, *62*, 6831−6836.

(8) Padera, T. P.; Stoll, B. R.; Tooredman, J. B.; Capen, D.; di Tomaso, E.; Jain, R. K. Pathology: cancer cells compress intratumour vessels. *Nature* **2004**, *427*, 695.

(9) Jain, R. K.; Tong, R. T.; Munn, L. L. Effect of vascular normalization by antiangiogenic therapy on interstitial hypertension, peritumor edema, and lymphatic metastasis: insights from a mathematical model. *Cancer Res.* **2007**, *67*, 2729−2735.

(10) Jain, R. K. Normalization of tumor vasculature: an emerging concept in antiangiogenic therapy. *Science* **2005**, *307*, 58−62.

(11) Fukumura, D.; Jain, R. K. Tumor microvasculature and microenvironment: targets for anti-angiogenesis and normalization. *Microvasc. Res.* **2007**, *74*, 72−84.

(12) Homsi, J.; Daud, A. I. Spectrum of activity and mechanism of action of VEGF/PDGF inhibitors. *Cancer Control* **2007**, *14*, 285−294.

(13) Dickson, P. V.; Hamner, J. B.; Sims, T. L.; Fraga, C. H.; Ng, C. Y.; Rajasekeran, S.; Hagedorn, N. L.; McCarville, M. B.; Stewart, C. F.; Davidoff, A. M. Bevacizumab-induced transient remodeling of the vasculature in neuroblastoma xenografts results in improved delivery and efficacy of systemically administered chemotherapy. *Clin. Cancer Res.* **2007**, *13*, 3942−3950.

(14) Kano, M. R.; Komuta, Y.; Iwata, C.; Oka, M.; Shirai, Y. T.; Morishita, Y.; Ouchi, Y.; Kataoka, K.; Miyazono, K. Comparison of the effects of the kinase inhibitors imatinib, sorafenib, and transforming growth factor-beta receptor inhibitor on extravasation of nanoparticles from neovasculature. *Cancer Sci.* **2009**, *100*, 173−180.

(15) Ohta, M.; Kawabata, T.; Yamamoto, M.; Tanaka, T.; Kikuchi, H.; Hiramatsu, Y.; Kamiya, K.; Baba, M.; Konno, H. TSU68, an antiangiogenic receptor tyrosine kinase inhibitor, induces tumor vascular normalization in a human cancer xenograft nude mouse model. *Surg. Today* **2009**, *39*, 1046−1053.

(16) Tailor, T. D.; Hanna, G.; Yarmolenko, P. S.; Dreher, M. R.; Betof, A. S.; Nixon, A. B.; Spasojevic, I.; Dewhirst, M. W. Effect of pazopanib on tumor microenvironment and liposome delivery. *Mol. Cancer Ther.* **2010**, *9*, 1798−1808.

(17) Tong, R. T.; Boucher, Y.; Kozin, S. V.; Winkler, F.; Hicklin, D. J.; Jain, R. K. Vascular normalization by vascular endothelial growth factor receptor 2 blockade induces a pressure gradient across the vasculature and improves drug penetration in tumors. *Cancer Res.* **2004**, *64*, 3731−3736.

(18) Winkler, F.; Kozin, S. V.; Tong, R. T.; Chae, S. S.; Booth, M. F.; Garkavtsev, I.; Xu, L.; Hicklin, D. J.; Fukumura, D.; di Tomaso, E.; Munn, L. L.; Jain, R. K. Kinetics of vascular normalization by VEGFR2 blockade governs brain tumor response to radiation: role of oxygenation, angiopoietin-1, and matrix metalloproteinases. *Cancer Cell* **2004**, *6*, 553−563.

(19) Ansiaux, R.; Baudelet, C.; Jordan, B. F.; Crokart, N.; Martinive, P.; DeWever, J.; Grégoire, V.; Feron, O.; Gallez, B. Mechanism of reoxygenation after antiangiogenic therapy using SU5416 and its importance for guiding combined antitumor therapy. *Cancer Res.* **2006**, *66*, 9698−9704.

(20) Bäckman, U.; Svensson, A.; Christofferson, R. Importance of vascular endothelial growth factor A in the progression of experimental neuroblastoma. *Angiogenesis* **2002**, *5*, 267−274.

(21) Gelderblom, H.; Verweij, J.; Nooter, K.; Sparreboom, A. Cremophor EL: the drawbacks and advantages of vehicle selection for drug formulation. *Eur. J. Cancer* **2001**, *37*, 1590−1598.

(22) Eskens, F. A.; Verweij, J. The clinical toxicity profile of vascular endothelial growth factor (VEGF) and vascular endothelial growth factor receptor (VEGFR) targeting angiogenesis inhibitors; a review. *Eur. J. Cancer* **2006**, *42*, 3127−3139.

(23) Fong, T. A.; Shawver, L. K.; Sun, L.; Tang, C.; App, H.; Powell, T. J.; Kim, Y. H.; Schreck, R.; Wang, X.; Risau, W.; Ullrich, A.; Hirth, K. P.; McMahon, G. SU5416 is a potent and selective inhibitor of the vascular endothelial growth factor receptor (Flk-1/KDR) that inhibits tyrosine kinase catalysis, tumor vascularization, and growth of multiple tumor types. *Cancer Res.* **1999**, *59*, 99−106.

(24) Giles, F. J.; Cooper, M. A.; Silverman, L.; Karp, J. E.; Lancet, J. E.; Zangari, M.; Shami, P. J.; Khan, K. D.; Hannah, A. L.; Cherrington, J. M.; Thomas, D. A.; Garcia-Manero, G.; Albitar, M.; Kantarjian, H. M.; Stopeck, A. T. Phase II study of SU5416–a small-molecule, vascular endothelial growth factor tyrosine-kinase receptor inhibitor–in patients with refractory myeloproliferative diseases. *Cancer* **2003**, *97*, 1920−1928.

(25) Yoshizawa, Y.; Kono, Y.; Ogawara, K.; Kimura, T.; Higaki, K. PEG liposomalization of paclitaxel improved its *in-vivo* disposition and anti-tumor efficacy. *Int. J. Pharm.* **2011**, *412*, 132−141.

(26) Lee, E. S.; Na, K.; Bae, Y. H. Doxorubicin loaded pH-sensitive polymeric micelles for reversal of resistant MCF-7 tumor. *J. Controlled Release* **2005**, *103*, 405−418.

(27) Horowitz, A.; Simons, M. Branching morphogenesis. *Circ. Res.* **2008**, *103*, 784−795.

(28) Carmeliet, P.; Ferreira, V.; Breier, G.; Pollefeyt, S.; Kieckens, L.; Gertsenstein, M.; Fahrig, M.; Vandenhoeck, A.; Harpal, K.; Eberhardt,

C.; Declercq, C.; Pawling, J.; Moons, L.; Collen, D.; Risau, W.; Nagy, A. Abnormal blood vessel development and lethality in embryos lacking a single VEGF allele. *Nature* **1996**, *380*, 435−439.
(29) Ellis, L. M.; Hicklin, D. J. VEGF-targeted therapy: mechanisms of anti-tumour activity. *Nat. Rev. Cancer* **2008**, *8*, 579−591.
(30) Crawford, Y.; Ferrara, N. VEGF inhibition: insights from preclinical and clinical studies. *Cell Tissue Res.* **2009**, *335*, 261−269.
(31) Maeda, H.; Wu, J.; Sawa, T.; Matsumura, Y.; Hori, K. Tumor vascular permeability and the EPR effect in macromolecular therapeutics: a review. *J. Controlled Release* **2000**, *65*, 271−284.
(32) Folkman, J. Tumor angiogenesis: therapeutic implications. *N. Engl. J. Med.* **1971**, *285*, 1182−1186.
(33) Díaz-Flores, L.; Gutiérrez, R.; Madrid, J. F.; Varela, H.; Valladares, F.; Acosta, E.; Martín-Vasallo, P.; Díaz-Flores, L., Jr. Pericytes. Morphofunction, interactions and pathology in a quiescent and activated mesenchymal cell niche. *Histol. Histopathol.* **2009**, *24*, 909−969.
(34) Ozawa, M. G.; Yao, V. J.; Chanthery, Y. H.; Troncoso, P.; Uemura, A.; Varner, A. S.; Kasman, I. M.; Pasqualini, R.; Arap, W.; McDonald, D. M. Angiogenesis with pericyte abnormalities in a transgenic model of prostate carcinoma. *Cancer* **2005**, *104*, 2104−2115.
(35) Baluk, P.; Hashizume, H.; McDonald, D. M. Cellular abnormalities of blood vessels as targets in cancer. *Curr. Opin. Genet. Dev.* **2005**, *15*, 102−111.
(36) Kalluri, R.; Zeisberg, M. Fibroblasts in cancer. *Nat. Rev. Cancer* **2006**, *6*, 392−401.
(37) Erber, R.; Thurnher, A.; Katsen, A. D.; Groth, G.; Kerger, H.; Hammes, H. P.; Menger, M. D.; Ullrich, A.; Vajkoczy, P. Combined inhibition of VEGF- and PDGF-signaling enforces tumor vessel regression by interfering with pericytes-mediated endothelial survival mechanisms. *FASEB J.* **2003**, *18*, 338−340.
(38) Kaluz, S.; Kaluzová, M.; Liao, S. Y.; Lerman, M.; Stanbridge, E. J. Transcriptional control of the tumor- and hypoxia-marker carbonic anhydrase 9: A one transcription factor (HIF-1) show? *Biochim. Biophys. Acta* **2009**, *1795*, 162−172.
(39) Stohrer, M.; Boucher, Y.; Stangassinger, M.; Jain, R. K. Oncotic pressure in solid tumors is elevated. *Cancer Res.* **2000**, *60*, 4251−4255.
(40) Padera, T. P.; Stoll, B. R.; Tooredman, J. B.; Capen, D.; di Tomaso, E.; Jain, R. K. Pathology: cancer cells compress intratumour vessels. *Nature* **2004**, *427*, 695.
(41) Helmlinger, G.; Yuan, F.; Dellian, M.; Jain, R. K. Interstitial pH and pO_2 gradients in solid tumors in vivo: high-resolution measurements reveal a lack of correlation. *Nat. Med.* **1997**, *3*, 177−182.
(42) Greenberg, J. I.; Shields, D. J.; Barillas, S. G.; Acevedo, L. M.; Murphy, E.; Huang, J.; Scheppke, L.; Stockmann, C.; Johnson, R. S.; Angle, N.; Cheresh, D. A. A role for VEGF as a negative regulator of pericyte function and vessel maturation. *Nature* **2008**, *456*, 809−813.
(43) Thurston, G.; Rudge, J. S.; Ioffe, E.; Zhou, H.; Ross, L.; Croll, S. D.; Glazer, N.; Holash, J.; McDonald, D. M.; Yancopoulos, G. D. Angiopoietin-1 protects the adult vasculature against plasma leakage. *Nat. Med.* **2000**, *6*, 460−463.
(44) Saharinen, P.; Eklund, L.; Miettinen, J.; Wirkkala, R.; Anisimov, A.; Winderlich, M.; Nottebaum, A.; Vestweber, D.; Deutsch, U.; Koh, G. Y.; Olsen, B. R.; Alitalo, K. Angiopoietins assemble distinct Tie2 signalling complexes in endothelial cell-cell and cell-matrix contacts. *Nat. Cell Biol.* **2008**, *10*, 527−537.
(45) Augustin, H. G.; Koh, G. Y.; Thurston, G.; Alitalo, K. Control of vascular morphogenesis and homeostasis through the angiopoietin-Tie system. *Nat. Rev. Mol. Cell Biol.* **2009**, *10*, 165−177.
(46) Stoeltzing, O.; Ahmad, S. A.; Liu, W.; McCarty, M. F.; Wey, J. S.; Parikh, A. A.; Fan, F.; Reinmuth, N.; Kawaguchi, M.; Bucana, C. D.; Ellis, L. M. Angiopoietin-1 inhibits vascular permeability, angiogenesis, and growth of hepatic colon cancer tumors. *Cancer Res.* **2003**, *63*, 3370−3377.
(47) Gaengel, K.; Genové, G.; Armulik, A.; Betsholtz, C. Endothelial-mural cell signaling in vascular development and angiogenesis. *Arterioscler., Thromb., Vasc. Biol.* **2009**, *29*, 630−638.
(48) Jain, R. K.; Stylianopoulos, T. Delivering nanomedicine to solid tumors. *Nat. Rev. Clin. Oncol.* **2010**, *7*, 653−664.
(49) Griffin, R. J.; Molema, G.; Dings, R. P. Angiogenesis treatment, new concepts on the horizon. *Angiogenesis* **2006**, *9*, 67−72.
(50) Ogawara, K.; Un, K.; Minato, K.; Tanaka, K.; Higaki, K.; Kimura, T. Determinants for *in vivo* anti-tumor effects of PEG liposomal doxorubicin: importance of vascular permeability within tumors. *Int. J. Pharm.* **2008**, *359*, 234−240.
(51) Chauhan, V. P.; Stylianopoulos, T.; Martin, J. D.; Popović, Z.; Chen, O.; Kamoun, W. S.; Bawendi, M. G.; Fukumura, D.; Jain, R. K. Normalization of tumour blood vessels improves the delivery of nanomedicines in a size-dependent manner. *Nat. Nanotechnol.* **2012**, *7*, 383−388.